The Wind Problem in COADS and Its Influence on the Water Balance

Zhongxiang Wu and Reginald E. Newell
Department of Earth, Atmospheric and Planetary Sciences, 54-1824
Massachusetts Institute of Technology
Cambridge, MA 02139

1. Introduction

The Comprehensive Ocean-Atmosphere Data Set (COADS) is the most complete data set available for the global oceanic regions up to now. Furthermore the data are updated almost in real time. Since the 1980s, 1.2 million ship observations have been collected for each new year, and the number for each year increases as more late data is collected until it reaches about 2.1 million reports. The data set provides us a great opportunity to reanalyze the behavior of the atmosphere and the oceans over the 70% of the surface which is poorly understood because of the lack of data. However, there are some problems in the data set since the observations were made over the global oceans by so many ships of different countries over such a long time span. Systematic trends in the reported winds is one of these problems. Ramage (1987) found that the scalar wind decreased between 1854 and 1920 and increased since World War II. He thought that the trends could be partly due to the transition from sailing ships to steamships and the method for making wind observations. Wright (1988) examined the trade winds in two regions and found similar trends; however the pressure gradient and rainfall data provide no support for the changes of winds and he concluded that the trends are artificial. Cardone et al. (1990) used ship files from NOAA's National Climatic Data Center (NCDC), to study the wind problem. Their results show that the ship reports in the South China Sea, North Pacific and North Atlantic shipping lanes also show increasing trends during the past three decades. They related the trends to the differences between the wind speed estimated from the Beaufort scale and that measured by anemometers and to the ship height. After corrections using Cardone's scale, they find no wind trends.

Variation of wind is directly related to the change of evaporation over the ocean and therefore to the water cycle in the atmosphere. If the wind speed over the oceans increased 1.0 ms^{-1} in the last thirty years, the increase of evaporation would be about 93 $kg^{-2}yr^{-1}$ if the difference of the specific humidity between the sea surface and the marine air is assumed to be 2 g/kg. This increase indicates about 6% more precipitation over the globe if the water content in the atmosphere is kept in the same level and the averaged rainfall is 1 m/yr. Therefore the wind trend should be considered together with evaporation and water balance.

In this study, we will examine the wind trends over the globe and discuss the influence on the global water budget.

2. Data and Processing

The data used are Monthly Summaries Trimmed (MST) of COADS Release 1 (1985) which is updated to 1987. The data include 9 observed variables, and 10 derived variables which provide intermediate products very useful for calculations of latent or sensible heats and wind stress. The data coverage before 1949 is not good enough for a global analysis, therefore this study only includes the data after 1949. The percentage of the wind observations over the Pacific for the period of 1949 to 1979 is shown in Figure 1. Almost all grids and all months are sampled in the Pacific north of 20°N. Coverage is about 50% in the tropical region and 60 to 80% in the band between 20 to 40°S. There are big gaps in the region south of 30°S and east of 130°W in the South Pacific as well as in most oceanic areas south of 40°S. The data coverages are better in the Atlantic and Indian Ocean. The observation numbers for other variables used in this study are similar to those of the winds. For the period from 1980 to 1987, the data are usually better than the previous period.

The wind data on nine island stations in the Pacific was supplied on magnetic tape by Dr. Joe Elms of NOAA/NCDC, Asheville. In addition several coastal stations from "Monthly Climatic Data for the World" are also used to compare with the ship's observed data.

The wind trends of 15 regions in different locations and the wind trends of all grids whenever the data are good enough to evaluate the trend, are calculated using the least squares regression method. The coordinates of the 15 regions are given in Table 1. The latent heat over the ocean surface is also calculated using the bulk equation

$$Q_L = \rho C_e W(q_s - q_a) \tag{1}$$

Where ρ is the air density which depends on the air temperature and the surface pressure, C_e is the transport coefficient for water vapor which is determined by wind speed and stability of the atmosphere, and will be discussed further later, W is the scalar wind and q_s - q_a the difference of specific humidity between sea and air.

3. Wind Trends

Time series of wind anomalies for 15 regions are shown in Figure 2. An increasing trend of about 1.5 m/s for the 39-year period exists for all regions. Over tropical oceans the increases are close to the monthly and interannual variations of the wind speed except for the tropical central Pacific. The climatological wind speed for the tropical west Pacific is only about 5 m/s, but the increase from 1949 to 1987 is as large as 1.8 m/s or 35%. Similar situations occurred for the tropical Atlantic and Indian ocean. For middle and high latitudes, the increasing trends are also obvious even though the monthly variations and interannual fluctuations are much larger than those of low latitudes. The largest trend occurs in the north central Pacific where the wind increase is more than 2.0 m/s, roughly 20% of the wind speed climatology.

Figure 3 shows the geographic distributions of the wind trends for the Pacific. They are quite space coherent in the regions with a high percentage of observations such as the north Pacific, a similar situation exists for the north Atlantic and most of the Indian Ocean, but there is a lack of coherence in the regions with poor observations such as south of 40°S (see figure 1). Increasing trends of 1 to 1.5 m/s exist almost everywhere. The trends are the largest in the northern part of the North Pacific and the middle of the South Indian Ocean, about 2 m/s, and are relatively small in the North Atlantic. The figure shows clearly that the trends are not limited locally but are a global phenomenon.

For such a global scale wind increase, the pressure field should show corresponding changes. An additional 1.9 hPa/1000 km of pressure gradient is necessary for a 1.5 m/s wind increase in 45° latitude. Therefore the mean pressure gradient fields for the periods from 1949 to 1953 and from 1983 to 1987 are calculated using the pressure data in COADS. The gradient differences between these two periods for the Pacific are given in Figure 4. Most grids show a slight decrease from the early to the recent period except in the high latitudes where the sampling is poor. A similar situation exists for the Pacific and Indian Ocean. The pressure field is not consistent with the wind trends. Wind observations in selected island and coastal stations, shown in Figure 5, are also inconsistent with the ship data. Large fluctuations with periods longer than 10 years show clearly at Adak and Hilo which might be real climatic variations, and big discontinuities at Truk, Yap and Shanghai which might be related to the instruments or method of observations. However increasing trends like those in figure 2 are difficult to find.

Most wind data in COADS are obtained from ship observations. Among these observations, the ratio of the number of observations which made use of estimated wind speed from the Beaufort scale to the number which used measured wind speed from anemometers increased gradually from less than 10% in the early 1950s to about 80% in the later 1980s (Ramage, 1987). The transformation from Beaufort scale to wind speed is based on the WMO Code 1100 (WMO, 1970). The basic formula used in the code is

$$v = c \bullet n^k \tag{2}$$

where v is wind speed in m/s and n is Beaufort number. The empirical values of c and k were originally determined in 1906 based on observations made on the little island of St. Mary's (Scilly), and adopted by WMO as an international scale in 1946. However it was soon found that the wind speed observed in the Scilly Isles is 2 m/s lower in Beaufort number 3 and 2 m/s higher in Beaufort number 9 than those observed on moving ocean ships and ocean weather ships. In 1960, members of the CMM (Commission for Maritime Meteorology) began to investigate the problem. Based on the 25 sets which already existed and 5 new sets of equivalent wind speed to the Beaufort scale, CMM proposed a new scale (CMM-IV) which was adopted by WMO in 1970 as a scientific scale but not used for operational purposes.
Another two scales were developed by Cardone in 1969 and Kaufeld in 1981 (Cardone, 1990, Isemer and Hasse, 1991). These two scales are very close to each other, but a little larger than the CMM-IV scale.

The CMM-IV scale is used to adjust the wind in this study. Since the monthly average data no longer includes the information of individual observations, we have to assume that the ratios of estimated to measured wind are the same for all grids during a certain year. Table 2 is used to find the corresponding wind speed on the CMM-IV scale for the part of the estimated wind. Since the CMM-IV scale is based on a ship height of 15-25 m and the coefficients used in the calculation of surface fluxes are related to the wind at a height of 10 m, the wind is further adjusted to this height using the formula

$$\frac{U_z}{u_*} = \frac{1}{k}\ln\left(\frac{z}{z_o}\right) \tag{3}$$

where u* is friction velocity, K the von Karman constant and z_o is roughness length. z_o and u* are related through the Charnock formula (Smith, 1980, Wu, 1980)

$$\frac{z_o}{u_*^2/g} = a \tag{4}$$

where a is constant and equal to 0.0185. ne Newton iterative method is applied to the above two equations to find z_o then using the roughness length, to calculate the wind at 10 m

The time series after the Beaufort scale and the height adjustment made are given in Figure 6. The trends are greatly reduced compared with figure 2. The trends in 14 of 15 regions almost disappear if the period after 1955 is considered. There is still a large trend in the northern central Pacific even though it has been greatly reduced. For this region, the wind speed increased 1 m/s rapidly from 1949 to 1953 and slowly from 1975 to 1987. Increasing trends also still exist in most regions before 1955. The trend for each grid after adjustment is given in Figure 7. The trends are much smaller than before adjustment. In most Atlantic regions the trends are within 0.5 m/s, which may be the noise level for such a complicated data set. There are still trends of more than 1 m/s in the region of 35-55°N in the North Pacific, which cannot be contributed by the sampling problem since there are more than 99%. Hence the adjustments used here solve part but not all observations reported of the whole problem.

Kaufeld’s scale has also been used to adjust the wind speed. The results are not significantly different from the results shown above as far as the trend problem is concerned, but would lead to more imbalance of the water budget.

4. Water Balance

One good test for an oceanic wind formulation is that the global ocean water budget be in balance which will be the case if the excess of evaporation over the oceanic precipitation is just balanced by the river flow. In this section we combine evaporation (E) values computed with equation (1) using COADS winds and specific humidity values with precipitation (P) values by Jaeger (1976) and compare (E-P) with river flow values compiled by UNESCO (1978). Two sets of COADS winds were used: the original data and the adjusted data as described above. In addition comparisons are also made with E-P values reported by Budyko, (1974) and Baumgartner and Reichel (1975). Originally transport coefficients for equation 1 by Isemer and Hasse (1987) were used. However the difference between evaporation and precipitation turned out to be 60x 10^3 km^3

yr^{-1}, too large to balance the river and underground water flow of $47x10^3$ km^3 yr^{-1}. Therefore the coefficients from Large and Pond (1982) were used for neutral conditions. The coefficients for other conditions were adjusted following the original Isemer and Hasse ratios. Results are shown in Table 3. The UNESCO river flows are 44.7×10^3 km^3 yr^{-1} so that the use of the adjusted winds gives a much close agreement.

Another problem that arises when latent heat estimates are made is that wind values reported as zero by the ships yield no evaporation from equation (1) in spite of substantial specific humidity gradients. However, active convection induces local winds of variable direction which do not get included in the ships reports and these encourage evaporation. This weak wind problem has been treated for many years by including a factor a+b(v) in place of W in equation (1) and various techniques have been used to evaluate a and b. Beljaars and Miller (1990) have recently provided a new formulation for this weak wind case which they find produces a better agreement with reality in the European Center for Medium Range Weather Forecasting (ECMWF) forecast model. Our next step is to include their formulation in the assessments made above.

Acknowledgements

We thank Joe Elms for the island station data and acknowledge support from NOAA Grant NA 26GPOO21-01 and NSF Grant ATM-9106902.

References

Baumgartner, A. and Reichel, E., 1975: *The World Water Balance*, Elsevier Science Publishing Company, Amsterdam, 179 pp.

Beljaars, A. and Miller, M., 1990: The sensitivity of the ECMWF model to the parameterization of evaporation from the tropical oceans, Technical Memorandum 170.

Budyko, M.I., 1974: *Climate and Life*, International Geophysics Series, Vol. 18, Academic Press, N.Y., 508 pp.

Cardone, V.J., Greenwood, J.G. and Cane, M., 1990: On Trends in the Historical Marine Wind Data, *Journal of Climate*, **3**, 113-127.

Slutz, R.J., Lubker, S.J., Hiscox, J.D., Woodruff, S.D., Jenne, R.L., Joseph, D.H., Steurer, P.M., and Elms, J.D., 1985: *COADS, Comprehensive Ocean-Atmosphere Data Set, Release 1*. Climate Research Program, Environmental Research Laboratories, Boulder, Colorado 262pp.

Isemer, H., and Hasse, L., 1987: *The Bunker Climate Atlas of the North Atlantic Ocean. Vol. 2: Air-Sea Interactions*, Springer-Verlag, Berlin Heidelberg, 24 pp. with 207 charts and 37 figures.

Isemer, H.J. and Hasse, L., 1991: The Scientific Beaufort Equivalent Scale: Effects on the Wind Statistics and Climatological Air-Sea Flux Estimates in the North Atlantic Ocean, *Journal of Climate*, **4**, 819-836.

Jaeger, L., 1976: Monatskarten des Niederschlags für die ganze Erde. *Berichte des Deutschen Wetterdienstes*, **139** (Band 18) Offenbach, 38 pp.

Large, W., and Pond, S., 1982: Sensible and Latent Heat Flux Measurements Over the Ocean, *Journal of Physical Oceanography*, **12**, 464-482.

Ramage, C.S., 1987: Secular Change in the Reported Surface Wind Speeds Over the Ocean, *Journal of Climate and Applied Meteorology*, **26**, 525-528.

Smith, S.D., 19080: Wind Stress and Flux Over the Ocean in Gale Force Wind, *Journal of Physical Oceanography*, **10**, 709-726.

UNESCO, 1978: *World water balance and water resources of the earth*, UNESCO Press, Paris, 663 pp.

WMO, 1970: *The Beaufort Scale of the Wind Force, Report No. 3*, Geneva, Switzerland, pp. 22.

Wright, P.B., 88: On the Reality of Climatic Changes in Wind Over the Pacific, *Journal of Climatology*, **8**, 521-527.

Wu, J., 1980: Wind-stress coefficients over sea surface near neutral conditions - a revisit, *Journal of Physical Oceanography*, **10**, 727-740.

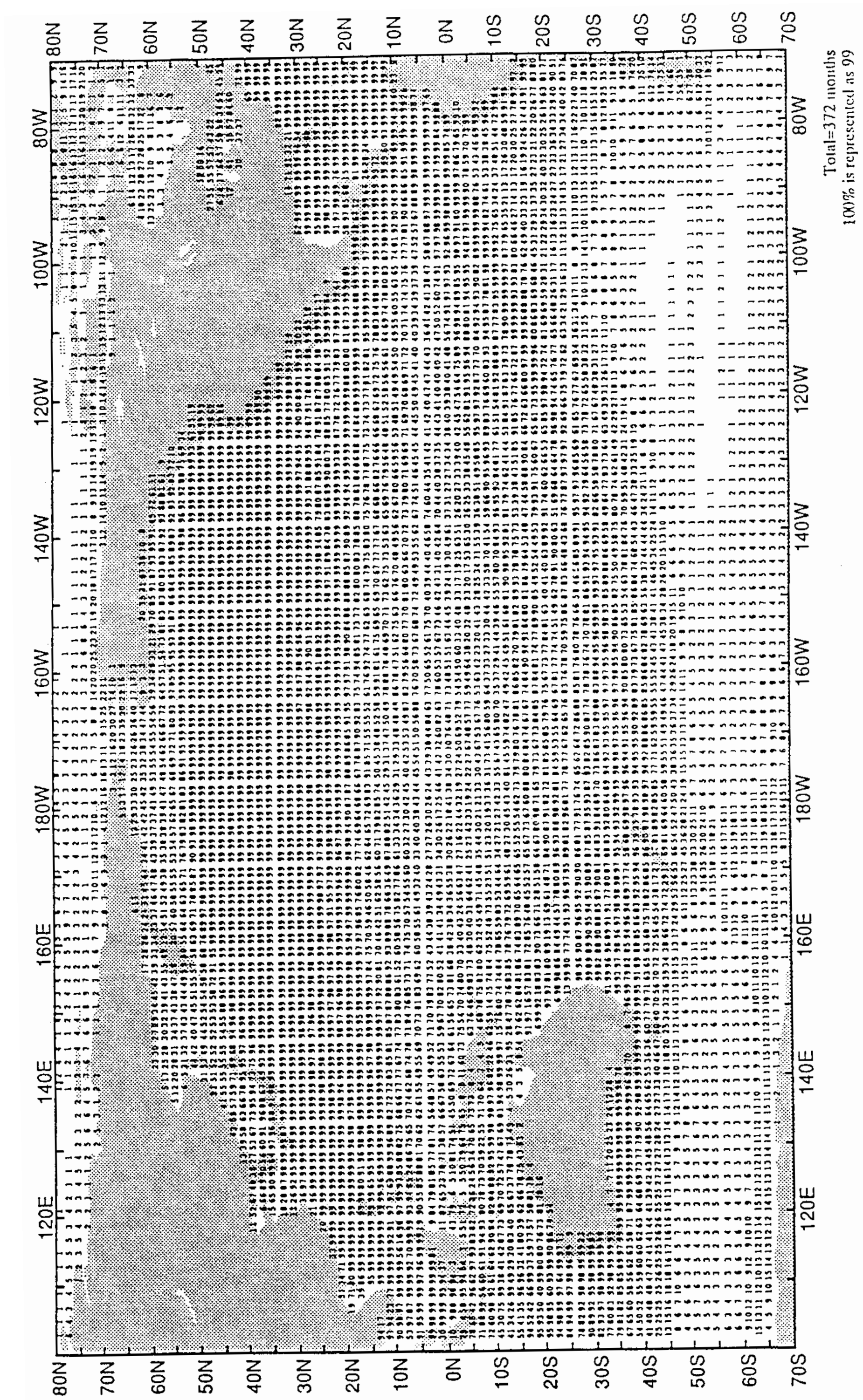

Figure 1. Percentage(%) of Wind Observation in Pacific Ocean, 1949-1979.

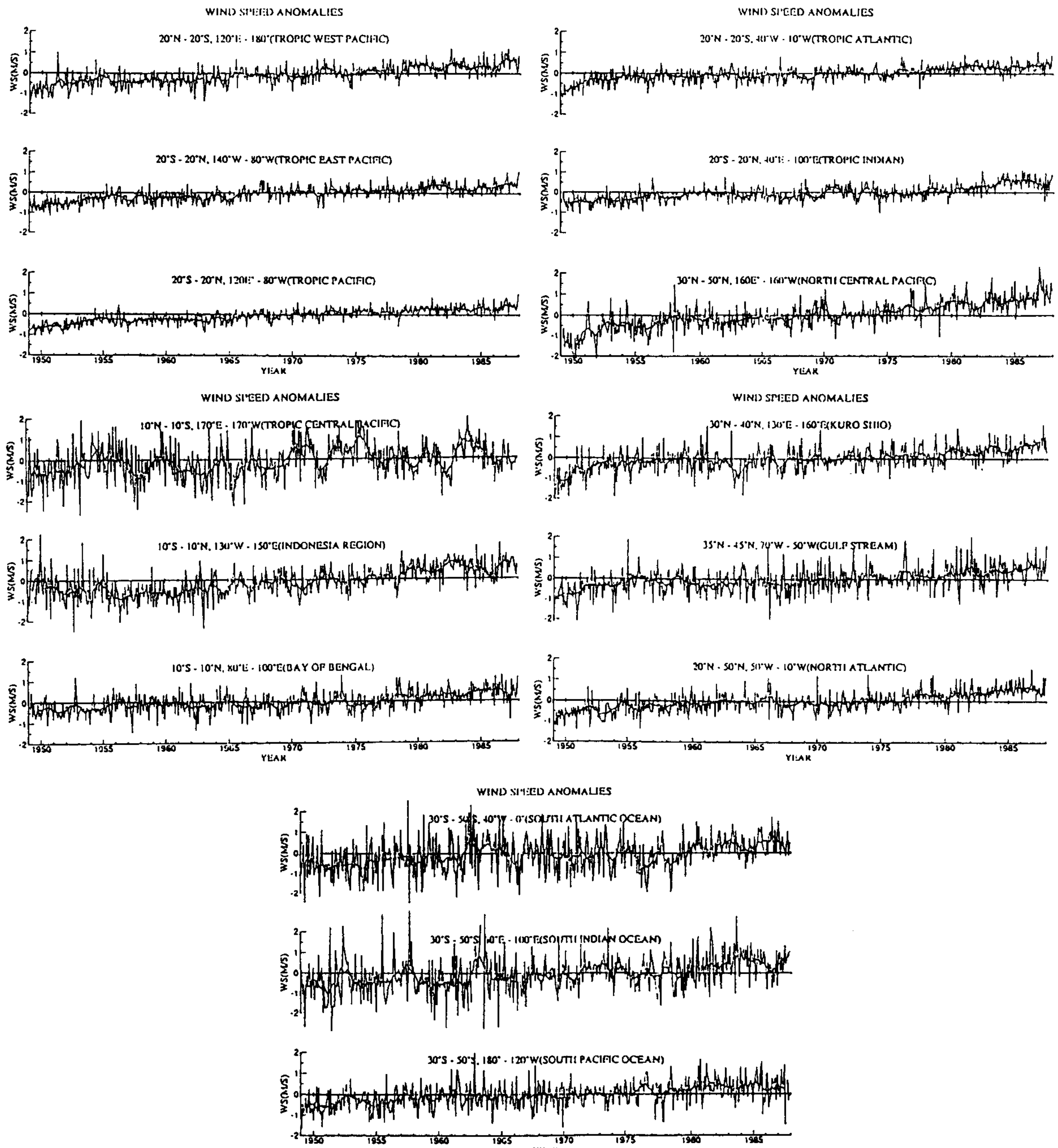

Figure 2. Time Series of Wind Speed Anomalies in 15 Selected Regions (Units m/sec^{-1}).

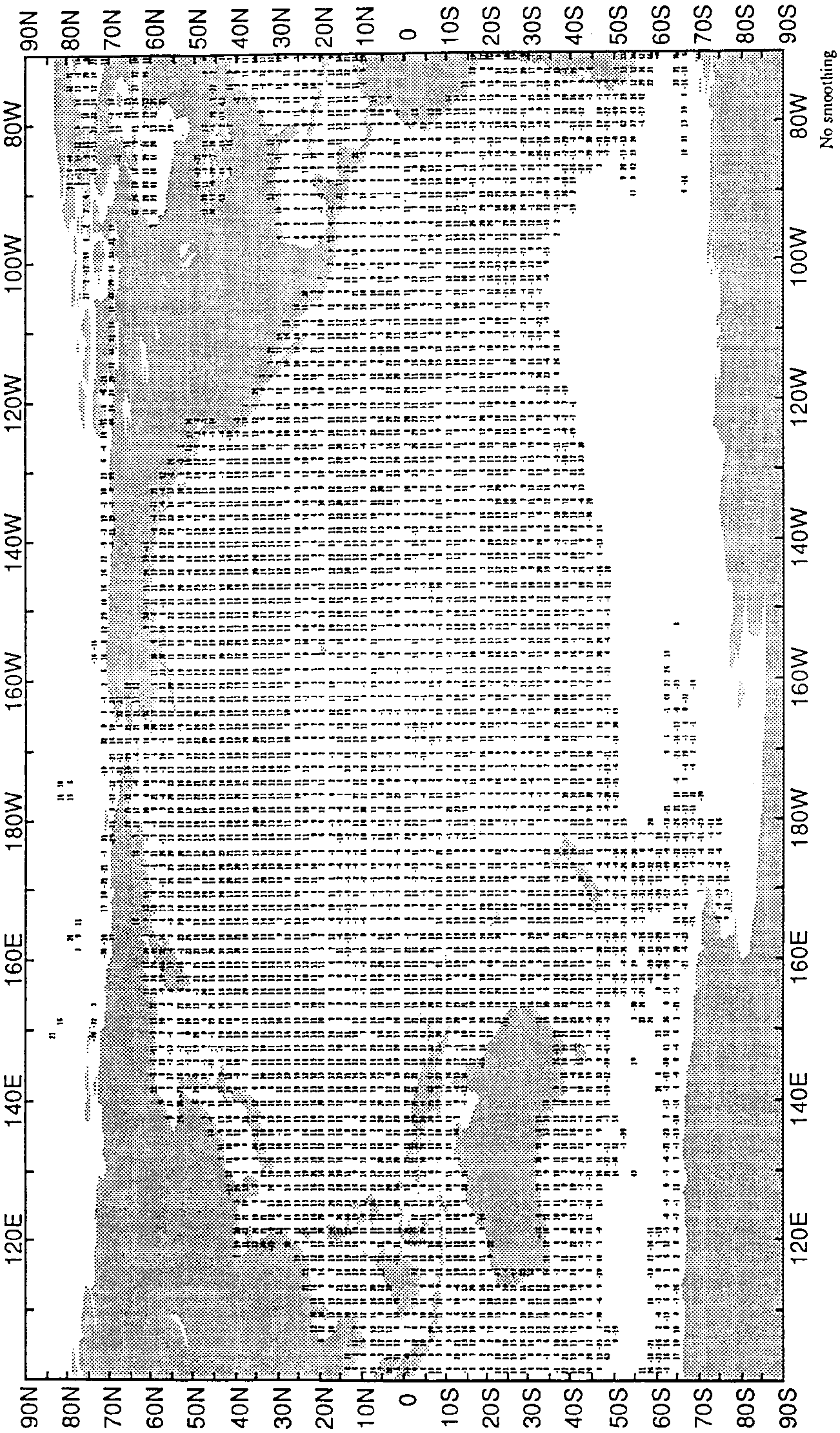

Figure 3. Pacific Wind Speed Trend (Units 0.1 m/s), 1949-1987.

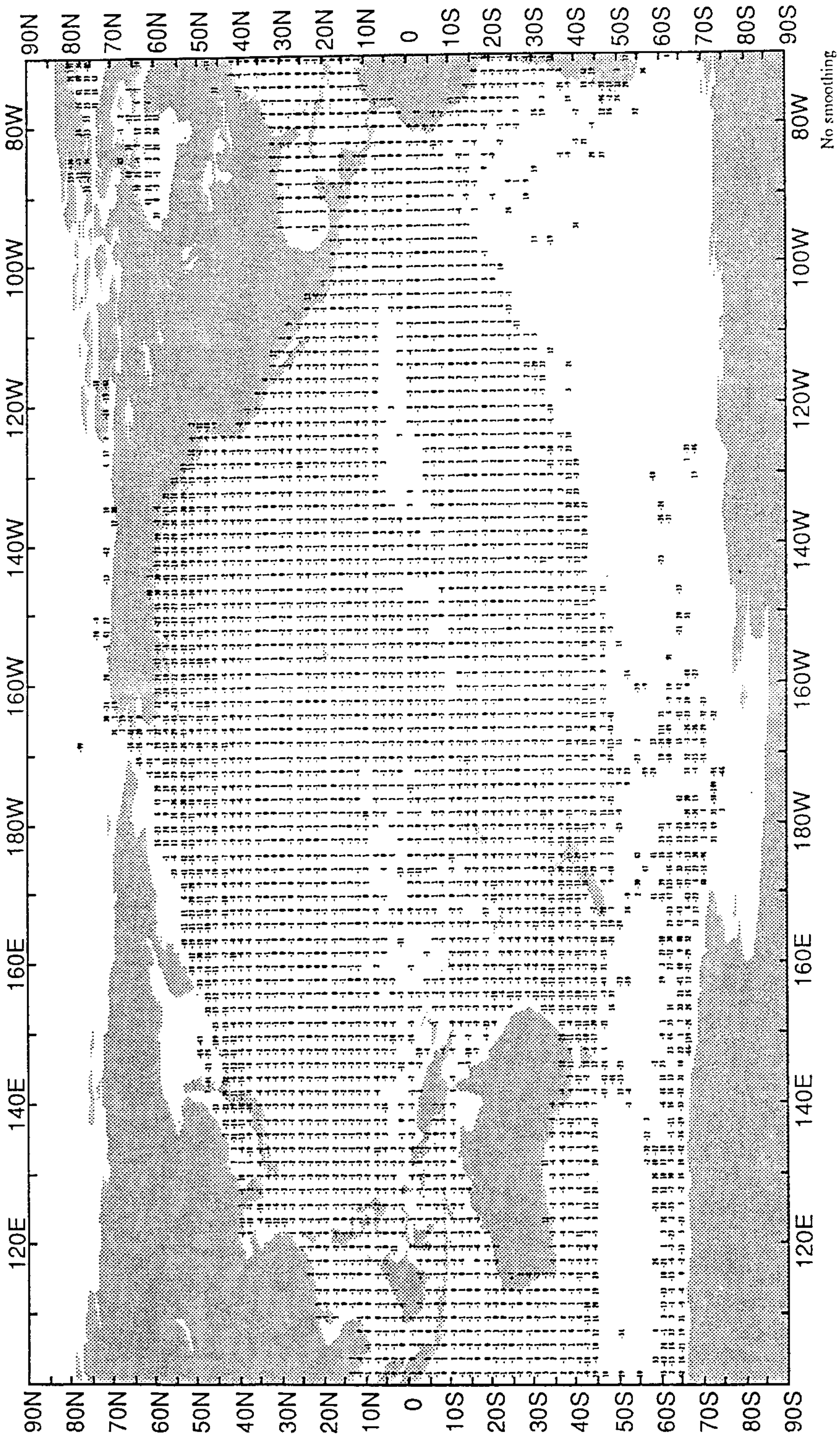

Figure 4. Differences of Pressure Gradients between the Period 1983-1987 and the Period 1949-1953.

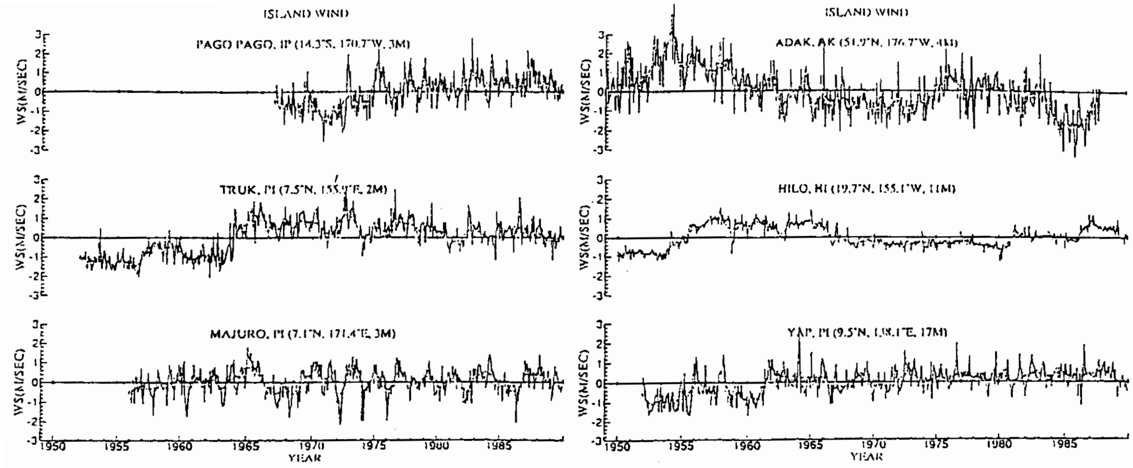

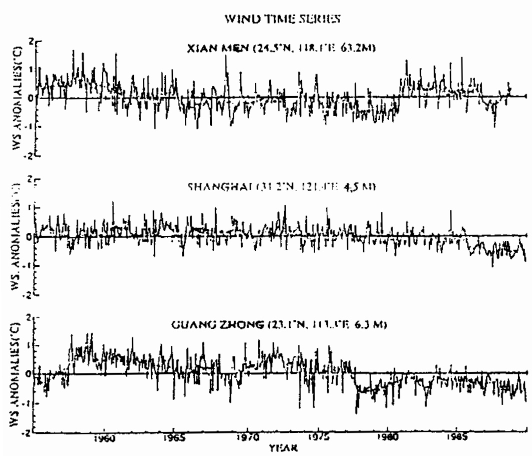

Table 1. Coordinates of the Regions

	Name of Region	Latitude (south negative)		Longitude (west negative)	
1	TROP. WEST PAC.	-20	20	120	180
2	TROP. EAST PAC.	-20	20	-140	-80
3	TROP. PACIFIC	-20	20	120	-80
4	TROP. CENT. PAC.	-10	10	170	-170
5	INDONESIA	-10	10	130	150
6	BAY OF BENGAL	-10	10	80	100
7	TROP. ATLANTIC	-20	20	-40	-10
8	TROP. INDIAN	-20	20	40	100
9	NORTH CENT. PAC.	30	50	160	-160
10	KURO SHIO	30	40	130	160
11	GULF STREAM	35	45	-70	-50
12	NORTH ATLANTIC	20	50	-50	-10
13	SOUTH ATLANTIC	-30	50	-40	0
14	SOUTH INDIAN	-30	-50	60	100
15	SOUTH PACIFIC	-30	-50	180	-120

Table 2. Comparison of WMO 1100 and CMM-IV Wind Speed Scales
Units: $msec^{-1}$

WMO1100	CMM-IV
0.0	0.8
0.8	2.0
2.4	3.6
4.3	5.6
6.7	7.8
9.4	10.2
12.3	12.6
15.5	15.1
18.9	17.8
22.6	20.8
26.4	24.2
30.5	28.0
34.9*	32.2

*Note:Including all wind speeds higher than this number.

Table 3. Evaporation (E), Precipitation (P) and (E-P) for oceans units: $10^3\ km^3\ yr^{-1}$

	PAC	ATL	IND	Globe
Evaporation (E)				
1) original winds	227	105	85	417
2) adjusted winds	221	102	84	408
3) Budyko	235	121	86	442
4) B and R	212	111	100	423
Precipitation (P)				
Jaegar	228	80	81	389
Budyko	235	87	91	413
B and R	228	74	81	385
E-P				
1) original winds	11.6	30.9	10.4	53.0
2) adjusted winds	5.7	28.4	9.4	43.5
3) Budyko	-1.7	34.3	11.6	43.9
4) B and R	-15.8	36.5	19.5	39.9

Baumgartner and Reichel

Figure 5. Time Series of Wind Speed Anomalies at 9 Stations.

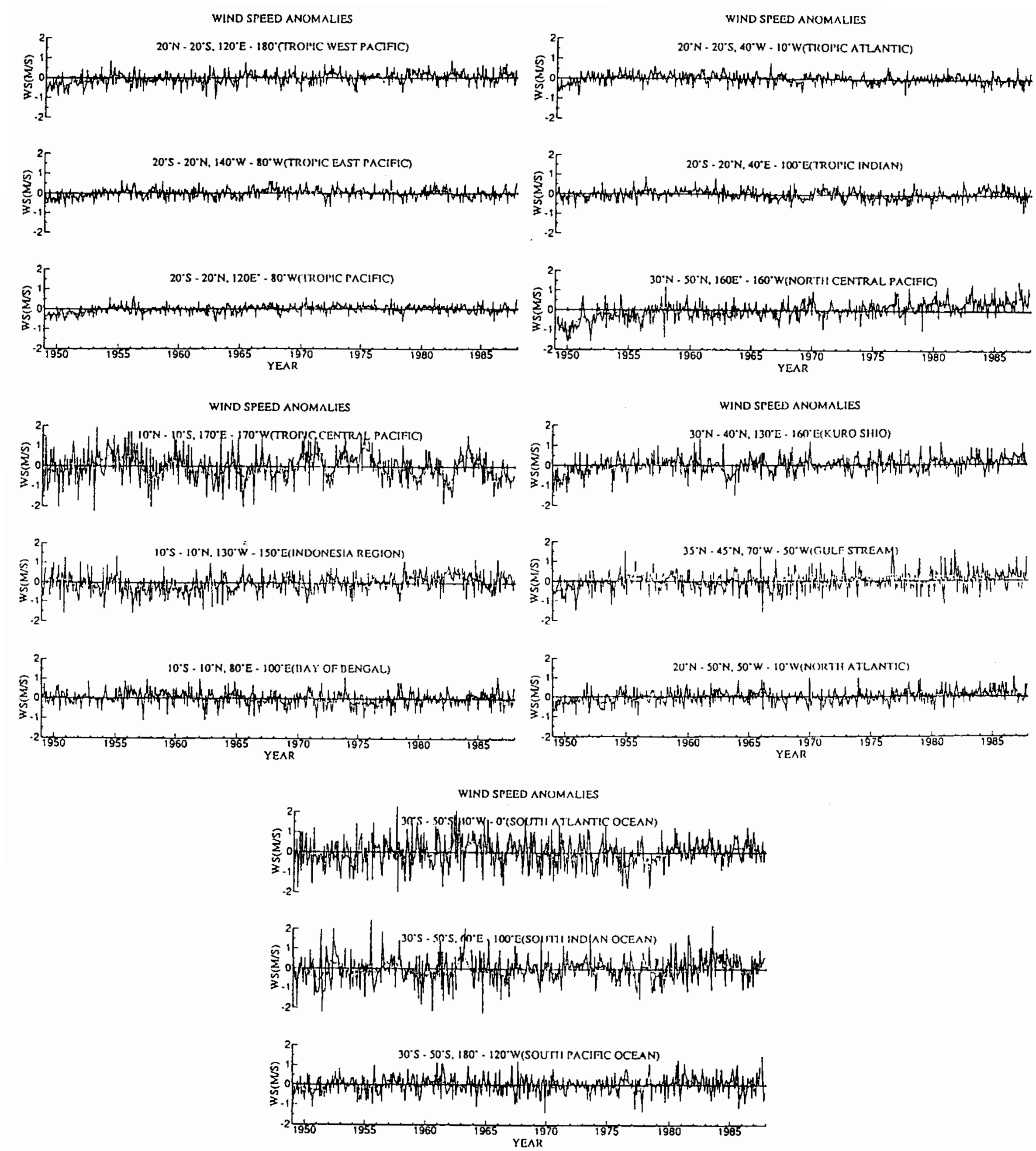

Figure 6. Same as Figure 2, but for the Corrected Time Series.

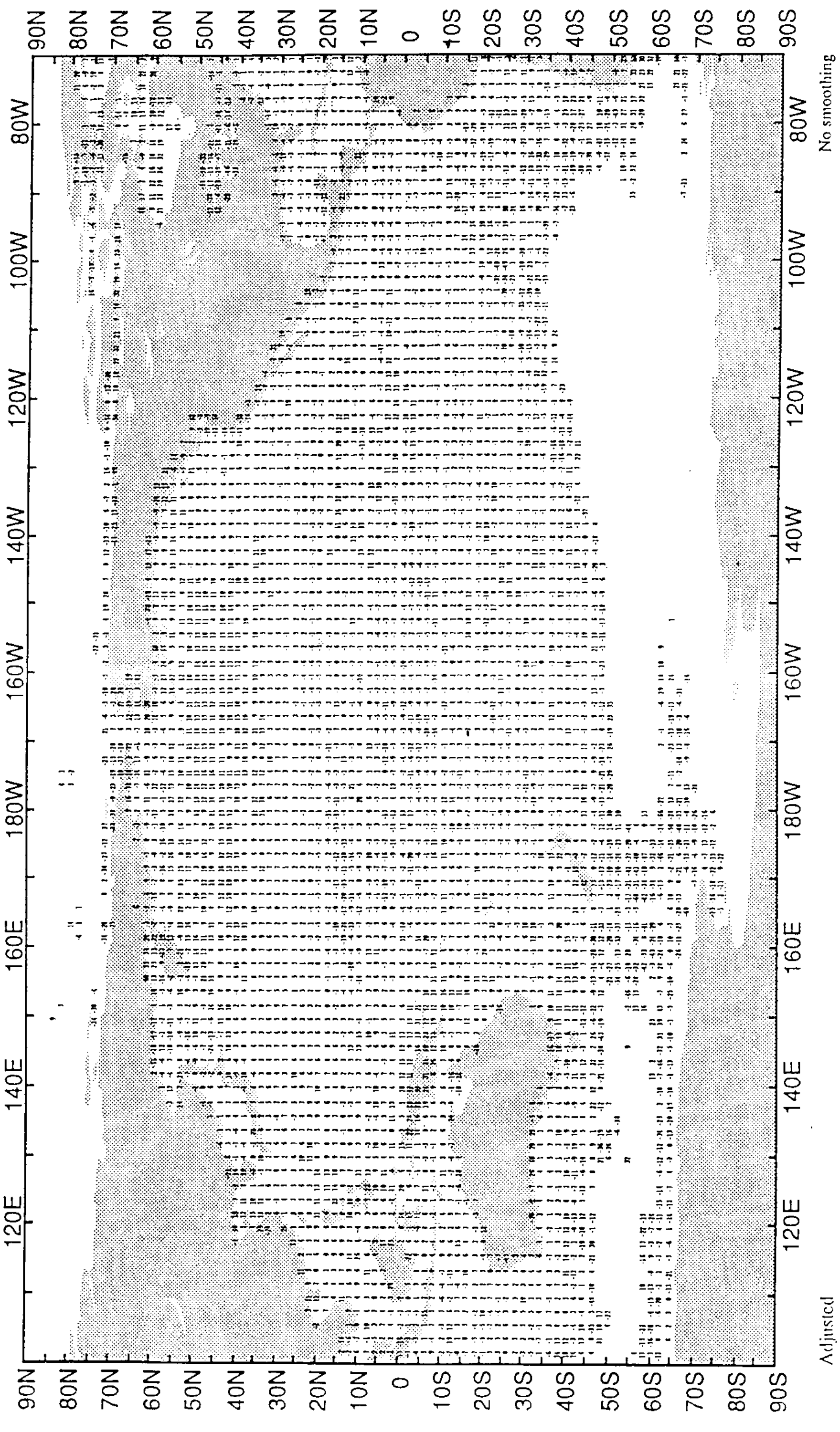

Figure 7. Same as Figure 3, but for the Corrected Wind.